Eur. Phys. J. B **18**, 319–327 (2000)

THE EUROPEAN PHYSICAL JOURNAL B

EDP Sciences
© Società Italiana di Fisica
Springer-Verlag 2000

A method for calculating the surface tension of a droplet in a lattice-gas model with long-range interaction

K. Ebihara[a] and T. Watanabe

Center for Computational Science and Engineering, Japan Atomic Energy Research Institute, Tokai-mura, Naka-gun, Ibaraki-ken, 319-1195, Japan

Received 15 March 2000 and Received in final form 31 May 2000

Abstract. Since the droplet of the lattice-gas model with long-range interaction is not circular and is determined by the Wulff construction due to surface tension anisotropy, a calculation method of the surface tension of the droplet is proposed in this paper. The calculated surface tension is in good agreement with the surface tension measured by using the Laplace's formula in consideration of the surface thickness.

PACS. 05.50+q Lattice theory and statistics (Ising, Potts, etc.) – 05.70.Fh Phase transitions: general studies – 68.10.Cr Surface energy (surface tension, interface tension, angle of contact, etc.)

1 Introduction

A lattice-gas model can simulate fluid as a many particle system. In the system of the 2D lattice-gas, particles are distributed on a triangular lattice and iterate propagation and collision [1,2]. The time evolution of the particle distribution is macroscopically similar to the fluid represented by the Navier-Stokes equations in the incompressible limit [1–3]. It is easier by using the lattice-gas model to simulate the flow in the system with complicated boundaries [2,4,5], such as the flow in porous media, than by using macroscopic hydrodynamics equations, because the boundary of the lattice-gas model can be imposed by restricting the particle existence on the node of the lattice. Multiphase flow can be also represented easily by the lattice-gas model because it is not necessary to consider the boundary condition at the interface between phases unlike the case of using the hydrodynamics equations [2,5].

There are two types of lattice-gas models which can represent the fluid system with phase separation. One is the immiscible lattice-gas model (ILG) [6–8] which can simulate the phase separation in the system consisting of more than one kind of component particle. The phase separation in the ILG model is caused by the attractive force among same kind of component particle. The other model [9–11] can represent the phase separation in the system consisting of one kind of component particle by adding the long-range interaction between particles. The phases which appear in the latter model have the different particle number density. This model obeys an equation of state similar to that of the liquid-vapor theory of van der Waals [12,13] and has the critical point (d_c, p_c, r_c) where d_c, p_c, and r_c are the critical particle density, the critical pressure and the critical distance of long-range interaction [14,15]. When the system is unstable and has the particle density less than the critical particle density, the high-density phase with the closed surface is generated in the phase with low density, that is a rare phase, like a droplet in vapor. In this paper, we call the lattice-gas model with long-range interaction and such generated dense phases in the rare phase the liquid-gas model [9,10,15] and the droplet, respectively.

Surface tension is one of the most important quantities in the system in which phase separation occurs because the surface tension influences the creation and annihilation of phases as well as the deformation of the interface between phases. The surface tension of the liquid-gas model has been discussed by several researchers [14,16–18]. Appert *et al.* [14] calculated the surface tension of the straight surface theoretically by using the probability distribution of the particle existence which depends on the coordinate normal to the interface. Appert and d'Humières [16] improved their calculation by introducing the probability distribution which depends on the particle velocity direction as well as the coordinate normal to the interface. Ebihara *et al.* [17] measured the surface tension of the droplet by using the Laplace's formula in consideration of the surface thickness. They also showed that the obtained surface tension was close to the surface tension of the straight surface which is not parallel to any of link directions of the lattice. Appert and Zaleski [18] showed surface tension anisotropy by measuring the surface tension of the straight surface and that the surface tension was adjustable by varying an arbitrary parameter. They also proposed the empirical equation for calculating the surface tension of the droplet. It was also shown that the surface tension of the droplet in the zero-curvature

[a] e-mail: ebihara@sugar.tokai.jaeri.go.jp

limit in which the radius of the mathematical circle fitting to the surface approaches infinity is in agreement with that of the straight surface [18].

The generated droplet of the liquid-gas model is not regarded exactly as the circular droplet because the surface shape in the system with surface tension anisotropy is in general determined by the Wulff construction [19]. Actually, the droplet shape of the liquid-gas model with the strong anisotropy of the surface tension is nearly hexagonal as it is seen in Section 3.1. Since the surface tension anisotropy depends on the position and the direction of the surface in the liquid-gas model, it cannot be considered that the surface tension of the droplet whose radius approaches infinity is not in agreement with that of the straight surface. In this paper, the surface tension of the droplet whose shape is determined by the Wulff construction is calculated by using the tension of two kinds of the straight surface. The calculated surface tension is compared with the surface tension which is measured by using the Laplace's formula in consideration of the surface thickness.

This paper is organized as follows. The liquid-gas model which is used in this paper is described in the next section. In Section 3, a calculation method of the surface tension of the droplet by using the tension of the straight surface without arbitrariness is proposed after the surface tension anisotropy of the liquid-gas model is described. In Section 4, first, the surface tension of two types of straight surfaces; one is parallel to one link of the lattice and the other is not parallel to any of links, is measured in numerical simulation. The surface tension on the straight surface which is parallel to one link is different from that on the straight surface which is not parallel to any links because of the surface tension anisotropy. It is found that the surface tension anisotropy is remarkable as the distance of the long-range interaction increases. Second, the surface tension of the droplet is measured by applying the Laplace's formula in consideration of the surface thickness and is compared with the surface tension which is calculated by the proposed method in Section 3. It is seen that both surface tensions of the droplet is in agreement with each other. It is verified that the difference between the surface tension of the straight surface and that of the droplet remains after the radius of the droplet approaches infinity. This paper is concluded in Section 5.

2 Liquid-gas model

The lattice-gas model which was proposed by Frisch, Hasslacher and Pomeau in 1986 (the FHP model) [1] can simulate fluid dynamics in the 2D system by the time evolution of the distribution of particles. The 2D space is discretized by the triangular lattice and the particles are distributed on the lattice nodes. The velocity direction of the particle is represented by the link, which connects nearest neighbor nodes, and its speed by the length of the link, that is the lattice constant. The equation of the time evolution in the macroscopic limit is similar to the incompressible Navier-Stokes equations [1–3]. The FHP model is classified according to its collision rules. Among FHP models, the FHP3 model is one of the most general models because this model involves all kinds of collisions which conserve local mass and momentum, that is the binary head-on and triple collisions and the dual collisions of them. The FHP3 model has the rest particle whose velocity is zero and the spectator particle which remains unaffected in collisions [3,20].

The equation of the time evolution is represented as

$$n_i(t+1, \mathbf{x}+\mathbf{c}_i) = n_i(t, \mathbf{x}) + \Delta_i[\mathbf{n}(t, \mathbf{x})], \tag{1}$$

where $\mathbf{n}(t, \mathbf{x}) = \{n_i(t, \mathbf{x})\}$ is the particle configuration at the node $\mathbf{x}$ and the step t, $n_i(t, \mathbf{x})$ takes 0 or 1, the index i which runs from 0 to 6 represents the velocity direction and $\mathbf{c}_i$ is the velocity vector

$$\mathbf{c}_i = (\cos[(i-1)\pi/6], \sin[(i-1)\pi/6]) \ (i = 1 \sim 6), \tag{2}$$

$$\mathbf{c}_0 = (0, 0). \tag{3}$$

In equation (1), $\Delta_i[\mathbf{n}(t, \mathbf{x})]$ is the collision term and satisfies $\sum_i \Delta_i[\mathbf{n}(t, \mathbf{x})] = 0$ due to mass conservation. Here three directions of the lattice-gas model are defined in Figure 1a. The direction along $\mathbf{c}_1$ is defined as the direction 1, which is parallel to the horizontal link. The direction along $\mathbf{c}_2$ is defined as the direction 2. The remained direction which is along $\mathbf{c}_3$ is defined as the direction 3. Applying the mean field approximation to equation (1) under the molecular chaos approximation, $\mathbf{n}(t, \mathbf{x})$ is replaced by the non-equilibrium particle distribution function $\mathbf{N}(t, \mathbf{x})$, so that the Boltzmann equation is obtained [2,3,15]. The non-equilibrium particle distribution function satisfies the following equations,

$$\rho(t, \mathbf{x}) = \sum_i N_i(t, \mathbf{x}), \quad \rho(t, \mathbf{x})\mathbf{u}(t, \mathbf{x}) = \sum_i \mathbf{c}_i N_i(t, \mathbf{x}), \tag{4}$$

where $\rho(t, \mathbf{x})$ is the local particle density and $\mathbf{u}(t, \mathbf{x})$ is the macroscopic velocity at $(t, \mathbf{x})$. By using the low-speed expansion and the multi-scale expansion (Chapman-Enskog expansion), the macroscopic equations similar to the incompressible Navier-Stokes equations are obtained [2,3].

The liquid-gas model was proposed by Appert and Zaleski [9]. While the collision rule of the FHP model satisfies the semi-detailed balance [14] as local mass and momentum conservation, the local momentum conservation is broken in the liquid-gas model by introducing the long-range interaction between particles. The phase separation occurs in the system including only one kind of component particle. The liquid-gas model can have several kinds of interactions [9,15,18]. In this paper, we use the liquid-gas model with five long-range interactions in Figure 1b which was proposed by Appert *et al.* [9]. These interactions have a good symmetry. In Figure 1b, the distance of long-range interaction is denoted by r. The equation of the time evolution (1) is modified as follows,

$$n'_i(t, \mathbf{x}) = n_i(t, \mathbf{x}) + L_i[\mathbf{n}(t, \mathbf{x}); r], \tag{5}$$

$$n_i(t+1, \mathbf{x}+\mathbf{c}_i) = n'_i(t, \mathbf{x}) + \Delta_i[\mathbf{n}'(t, \mathbf{x})], \tag{6}$$

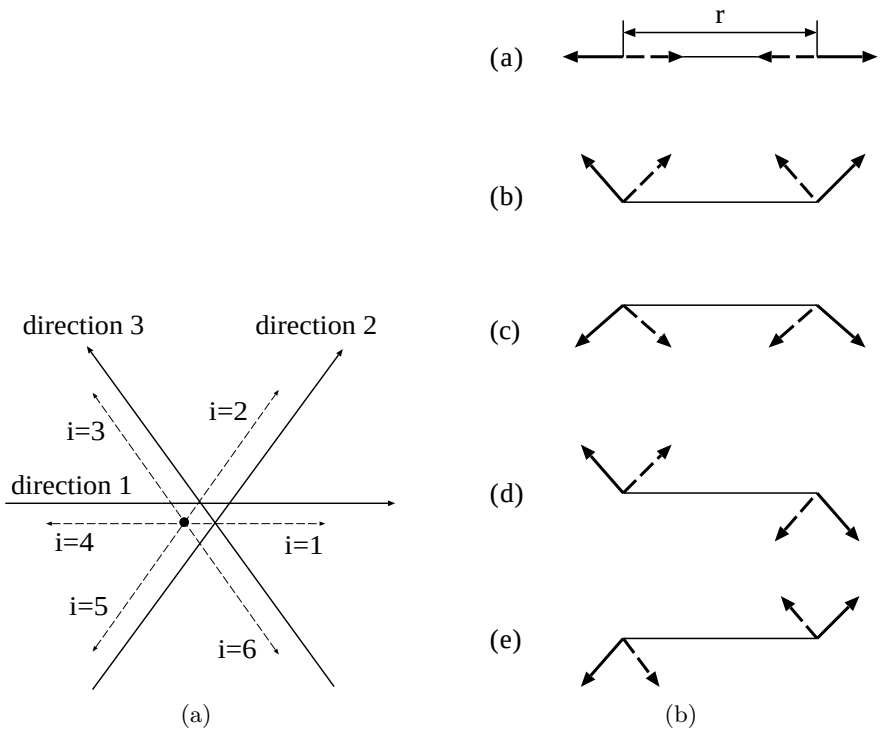

Fig. 1. (a) Link directions: The solid arrow means the direction of the link and the dashed arrow means the velocity direction. (b) Long-range interaction: The solid arrow means the site occupied by the particle and the dashed arrow means the hole site. This figure represents the configuration before applying the interaction. After the interaction, the solid arrow is exchanged with the dashed arrow. The interaction distance is denoted by r.

where $L_i[\mathbf{n}(t, \mathbf{x}); r]$ is the long-range interaction term. In the macroscopic limit, pressure, viscosity and sound speed are modified by adding the long-range interaction [2].

3 Surface tension of the droplet

First, the surface tension anisotropy of the liquid-gas model is described in this section. Next, the method to calculate the surface tension of the droplet in the liquid-gas model is proposed by considering the surface tension anisotropy. The surface tension calculated by this method is compared with that measured by using the Laplace's formula in consideration of the surface thickness.

3.1 Surface tension anisotropy

The surface tension anisotropy of the liquid-gas model is described by considering the surface tension of straight surfaces. The surface tension of the straight surface, σ, can be measured by using the following formula [21],

$$\sigma = \int_{-\infty}^{\infty} \{p_{\mathrm{n}} - p_{\mathrm{t}}(z)\} \mathrm{d}z, \tag{7}$$

where z is the direction normal to the surface, p_{n} and $p_{\mathrm{t}}(z)$ are the normal pressure and the tangential pressure to the surface. The pressure for the liquid-gas model is obtained from the momentum flux which is the momentum transferred by the particle propagation and the long-range interaction [14,15,18]. The momentum flux is measured on each lattice link. The measured momentum flux on each link is decomposed into the normal component and the tangential component for obtaining the normal and tangential pressure in equation (7) [14,18]. If the straight surface is parallel to one link direction, the transferred momentum in this link direction is different from that in the link direction which is not parallel to the surface because the particles which undergo the long-range interaction are in the same phase. Therefore the surface tension of the straight surface which is parallel to one link direction is different from that of the straight surface which is not parallel to any of link directions. This is the surface tension anisotropy of the liquid-gas model.

Because of the surface tension anisotropy of the liquid-gas model, it is considered that the shape of the generated droplet is determined by the Wulff construction. In Figure 2, two droplets in equilibrium are shown as the particle distribution in the 600×600 lattice system with $d = 0.17$. Here d means the reduced density which is obtained by dividing the particle number density of the system by the maximum number of particles in one node [2,3]. One is for $r = 9$ and the other for $r = 19$. In this figure, the tone of the dot changes gradually from dark to white as the particle density of the node decreases.

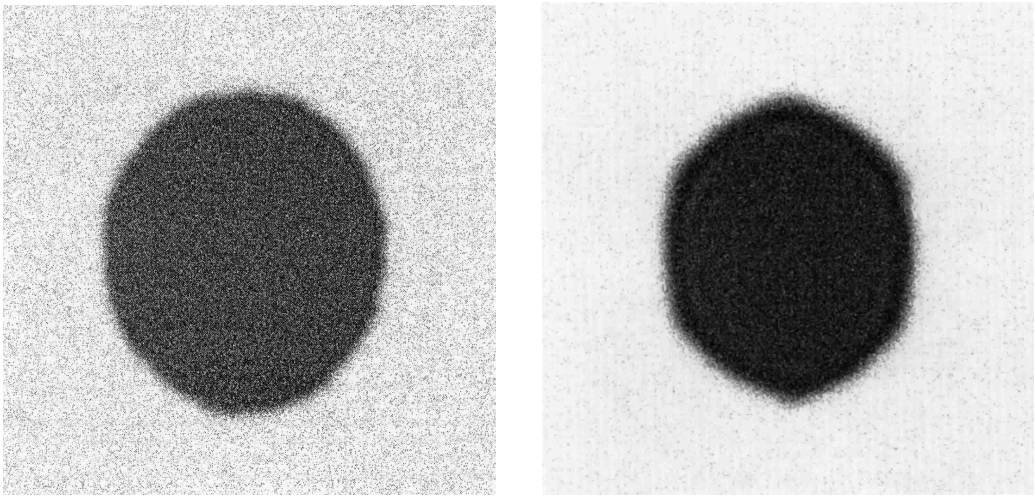

(a) (b)

Fig. 2. Droplets (a) for $r = 9$ and (b) for $r = 19$: Both droplets are generated in the 600×600 lattice system with $d = 0.17$. The tone of the dot changes gradually from dark to white as the density of the node decrease.

It is found in the figure that the droplet for $r = 19$ is deviated from the circle more clearly than that for $r = 9$.

3.2 Calculation method of the surface tension of the droplet

Generally, the surface in the system with surface tension anisotropy is determined by the Wulff construction and is not circular. Thus, it is considered that the surface of the droplet of the liquid-gas model consists of many pieces of small straight surfaces. On the basis of the discussion in Section 3.1, it is assumed that the liquid-gas model has two values of the surface tension according to the surface direction; one is the surface tension of the straight surface which is parallel to one link direction, $\sigma_{\parallel}$, and the other is that of the straight surface which is not parallel to any link direction, $\sigma_{\perp}$. By using these two surface tensions, the surface tension of the droplet, $\sigma_{\rm c}$, is represented by

$$\sigma_{\rm c} = \alpha_{\parallel}\sigma_{\parallel} + \alpha_{\perp}\sigma_{\perp} \tag{8}$$

where $\alpha_{\parallel}$ is the ratio of the length of the surface with the tangent parallel to one of three link directions to the length of the droplet surface and $\alpha_{\perp} = 1 - \alpha_{\parallel}$. The surface of the droplet is divided into the parallel part and the non-parallel part according to the relation between the tangent of the surface of the droplet and the link direction. This means that the surface tension of the droplet is represented by combining the tension of the straight surfaces. Thus it is necessary to define the tangent of the surface which is parallel to the link direction in the liquid-gas model.

The tangent of the surface which is parallel to the link direction is defined by considering the way of the pressure measurement in the liquid-gas model. As described in the Section 3.1, the pressure of the liquid-gas model is obtained from the momentum flux which is measured on the lattice link by counting the transferred momentum by the particle propagation and the long-range interaction. In order to calculate the surface tension of the droplet, it is necessary to obtain the momentum flux at a certain point. The momentum flux at a point is obtained by interpolating the momentum flux on links which surround the point concerned. The measurement of the momentum flux at the point is illustrated in Figure 3. According to the figure, the momentum flux at the point is determined by the particle configuration on the segments with $2r$ or $2r-1$ in length which surround the point concerned. If the point of contact of the tangent of the surface is considered as the point discussed above, the momentum flux at this point of contact changes due to the direction of the tangent. In other words, the relation between the tangent of the surface and the segments which surround its point of contact determines the momentum flux at the point of contact. When one of these segments is included in one of phases which are separated by the interface, the momentum flux is largely different from the momentum flux of the case that all of the segments intersect the interface. Therefore, for the liquid-gas model, when the tangent of the droplet surface does not intersect one of segments with $2r$ or $2r-1$ in length surrounding its point of contact, the tangent is defined to be parallel to the link direction along this segment. Examples of the definition of the parallel tangent of the surface of the droplet are illustrated in Figure 4.

According to this definition, the tangent parallel to the link direction is determined by the position of the point of contact, the slope of the tangent and the distance of the long-range interaction. Therefore the droplet surface can be divided into the parallel part and non-parallel part without any arbitrariness. Since the tangent of the surface of the droplet has any slope, the surface tension

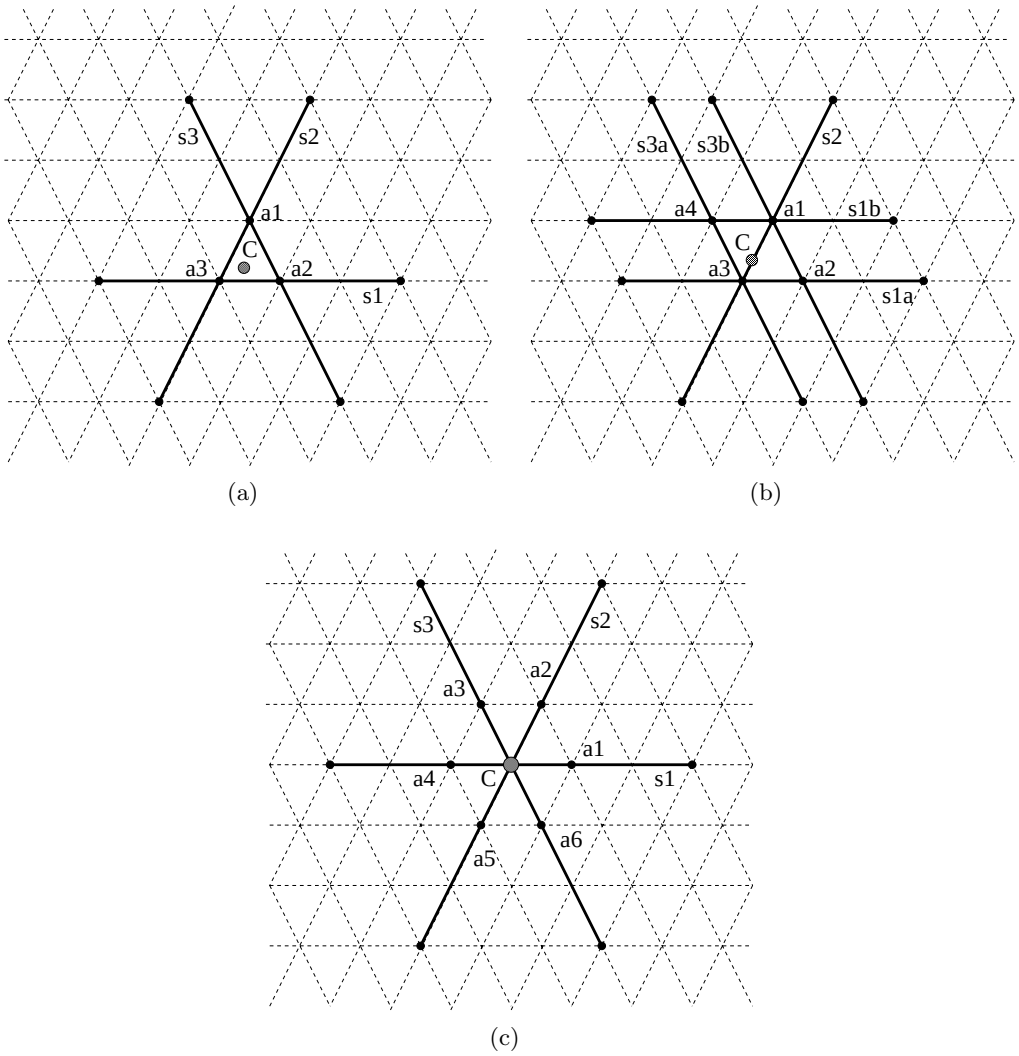

Fig. 3. Measurement of the momentum flux at a certain point: The point concerned is C. In these figures, the distance of the long-range interaction is considered as $r = 3$. (a) The point C is neither lattice links nor lattice nodes. The momentum flux at the point is obtained by interpolating the momentum flux on the links, a_1a_2, a_2a_3, and a_1a_3, which is determined by the particle configuration on the segments, s_1, s_2, and s_3, respectively. The length of these segments is $2r - 1 = 5$. (b) The point C is not on nodes but on the link, a_1a_3. The momentum flux at the point is obtained by interpolating the momentum flux on the links, a_1a_2, a_2a_3, a_1a_3, a_1a_4, and a_3a_4, which is determined by the particle configuration on the segments, s_{3b}, s_{1a}, s_2, s_{1b}, and s_{3a}, respectively. The length of these segments is also $2r - 1 = 5$. (c) The point C is on the node. The momentum flux at the point is obtained by interpolating the momentum flux on six links which surround this point. The momentum flux on links, Ca_1 and Ca_4, is determined by the particle configuration on the segment s_1, Ca_2 and Ca_5 is by s_2, Ca_3 and Ca_6 is by s_3, respectively. The length of these segments is $2r = 6$.

of the droplet is not in agreement with that of the straight surfaces if the radius of the droplet approaches infinity.

4 Numerical simulations

In this section, first, $\sigma_{\parallel}$ and $\sigma_{\perp}$ in equation (8) are measured on the straight surfaces. Next, the surface tension of the droplet is measured by using the Laplace's formula in consideration of the surface thickness and is compared with the surface tension which is calculated by using the method in the previous section.

4.1 Surface tension of the straight surface

In order to measure $\sigma_{\parallel}$ and $\sigma_{\perp}$, two straight surfaces of the dense phase which is generated on one wall of two parallel walls are used in the numerical simulation in the 600×600 lattice system with $d = 0.17$. One is parallel to the x-axis and the other is perpendicular to the x-axis. We call the former straight surface the horizontal straight surface and the latter the vertical straight surface. In Figure 5, both dense phases in equilibrium are shown as the particle distribution. The surface tension of both straight surfaces is measured by using equation (7).

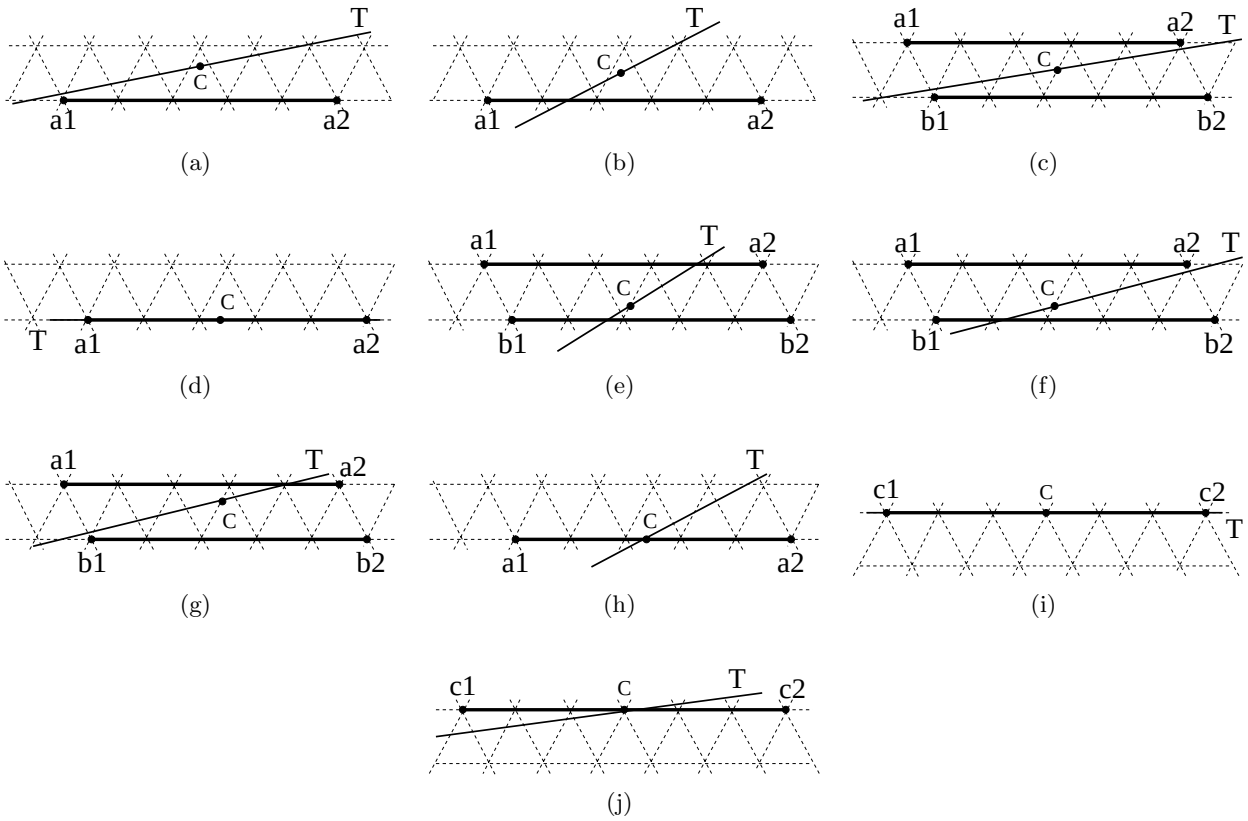

Fig. 4. Examples of the relation between the tangent and the segment along the link direction: T is the tangent and C is the point of contact. The segments, a_1a_2, b_1b_2, and c_1c_2, are along the direction 1. In these examples, the case of $r = 3$ is shown and $\overline{a_1a_2} = \overline{b_1b_2} = 2r - 1 = 5$ and $\overline{c_1c_2} = 2r = 6$. (a) and (b) are for the case that the point C is on neither the link nor the node. (c) $\sim$ (h) are for the case of that the point C is on the link. (i) and (j) are for the case of that the point C is on the node. (a), (c), (d), and (i) are examples of the tangent parallel to the direction 1 because the tangent intersects neither the segment a_1a_2 nor b_1b_2 nor c_1c_2. (b), (e), (f), (g), (h), and (j) are examples of the tangent which is not parallel to the direction 1 because the tangent intersects the segment.

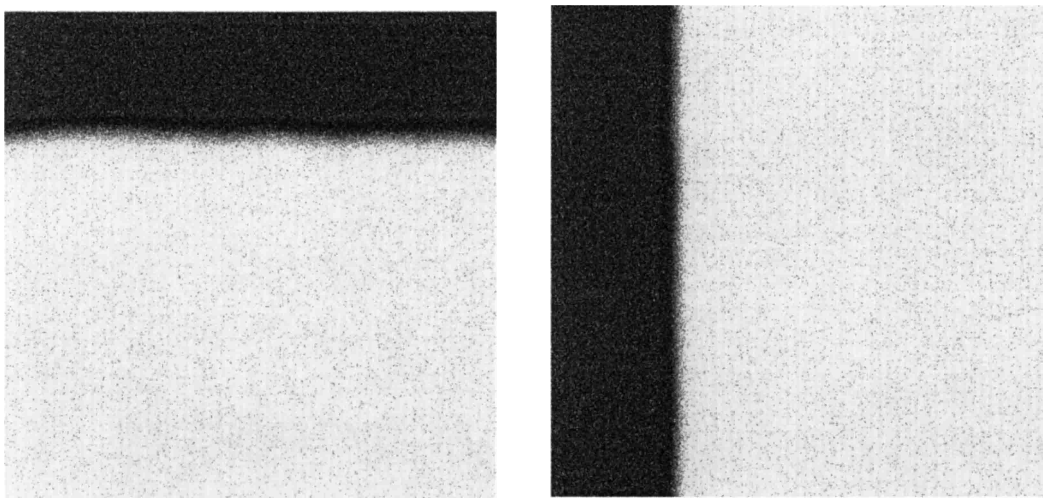

(a) (b)

Fig. 5. (a) Horizontal straight surface and (b) Vertical straight surface : Both dense phases are generated on one wall of two parallel walls in the 600×600 lattice system with $d = 0.17$ and $r = 15$. The tone of the dot changes gradually from dark to white as the density of the node decrease.

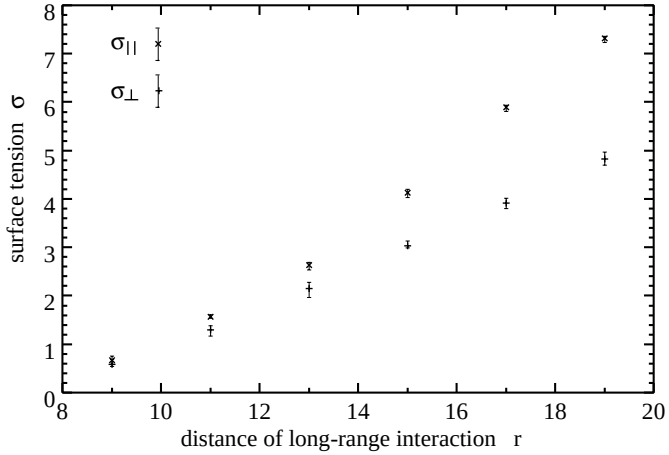

Fig. 6. Surface tensions of the horizontal straight surface and the vertical straight surface against the distance of the long-range interaction: The numerical simulation is carried out in the 600×600 lattice system with $d = 0.17$ for each r.

The pressure in equation (7) was obtained by averaging over 1200 steps in each simulation. The surface tension was obtained by averaging over 5 simulations. The measured surface tension on both straight surfaces is shown in Figure 6 for $r = 9$ to $r = 19$. It is seen that the surface tension of the horizontal straight surface is larger for each r than that of the vertical straight surface. It is found that the difference between the surface tension of both straight surfaces is remarkable as the distance of the long-range interaction increases.

4.2 Surface tension of the droplet

4.2.1 Determination of the surface position

In order to measure the surface tension of the droplet by using the Laplace's formula, it is necessary to define the surface position clearly.

Considering the interface between the dense phase and the rare phase, the profile of the density distribution $\rho(z)$ in the vicinity of the interface is ideally represented by using the dense-phase density, ρ_{D}, and the rare-phase density, ρ_{R}, in equilibrium as [21]

$$\rho(z) = \rho_{\mathrm{R}} + \frac{1}{2}(\rho_{\mathrm{D}} - \rho_{\mathrm{R}})\{1 - \tanh\zeta(z - R_s)\}, \qquad (9)$$

where ζ is an arbitrary steepness parameter, z is the direction from the dense phase to the rare phase and R_s is the interface position. The interface position, R_s, satisfies the equation,

$$\int_{-\infty}^{R_s}\{\rho_{\mathrm{D}} - \rho(z)\}\mathrm{d}z = \int_{R_s}^{\infty}\{\rho(z) - \rho_{\mathrm{R}}\}\mathrm{d}z. \qquad (10)$$

By replacing $\pm\infty$ with $R_s \pm \alpha$ in this equation where α is an arbitrary finite constant, the relation,

$$\frac{1}{2\alpha}\int_{R_s-\alpha}^{R_s+\alpha}\rho(z)\mathrm{d}z = \frac{1}{2}(\rho_{\mathrm{D}} + \rho_{\mathrm{R}}) \equiv \rho_{\mathrm{S}}, \qquad (11)$$

is obtained. This relation means that R_s can be represented by using ρ_{D} and ρ_{R} because α is arbitrary.

Table 1. Particle densities of the dense phase and the rare phase in equilibrium

r	ρ_{D}	ρ_{R}
9	$3.5329\ (\pm 4.61 \times 10^{-4})$	$0.2142\ (\pm 1.26 \times 10^{-3})$
11	$4.0369\ (\pm 8.54 \times 10^{-4})$	$0.1099\ (\pm 4.94 \times 10^{-4})$
13	$4.3743\ (\pm 7.63 \times 10^{-4})$	$0.0637\ (\pm 4.59 \times 10^{-4})$
15	$4.6228\ (\pm 3.64 \times 10^{-4})$	$0.0399\ (\pm 3.37 \times 10^{-4})$
17	$4.8153\ (\pm 7.49 \times 10^{-4})$	$0.0252\ (\pm 2.32 \times 10^{-4})$
19	$4.9707\ (\pm 3.02 \times 10^{-4})$	$0.0168\ (\pm 2.23 \times 10^{-4})$

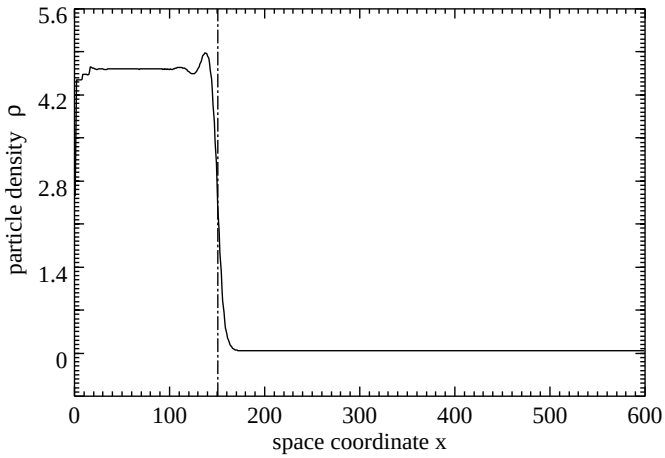

Fig. 7. Density profile of Figure 5b: The dash-dotted line represents the position of the interface

This relation is used for the determination of the surface position in the liquid-gas model. The density in the circle with the radius, r, whose center is the lattice node, ρ_{cir}, is measured and compared with ρ_{S}. If $\rho_{\mathrm{cir}} \geq \rho_{\mathrm{S}}$, the node at the center of the circle is considered as the node in the dense phase. If $\rho_{\mathrm{cir}} < \rho_{\mathrm{S}}$, the center node is in the rare phase. By applying this procedure to every node in the system, all of the nodes are classified into the dense phase or the rare phase. This method is called the local-region clustering method [17]. Then the node of the surface is obtained as the node in the dense phase which is next to the node in the rare phase.

Here it is necessary to measure the particle densities of the dense phase and of the rare phase in equilibrium, ρ_{D} and ρ_{R}, which are used in the local-region clustering method. Since ρ_{D} and ρ_{R} depend only on the distance of the long-range interaction, these are measured by generating the vertical dense phase on the wall as described in Section 3.1. In Figure 7, the particle density distribution of Figure 5b is shown as an example. The obtained density distribution changes abruptly in the vicinity of the interface and is almost constant in the dense-phase region and the rare-phase region except the region in the vicinity of the wall. The densities, ρ_{D} and ρ_{R}, are obtained by averaging over the region with the constant density respectively. The obtained density is shown for $r = 9$ to $r = 19$ in Table 1.

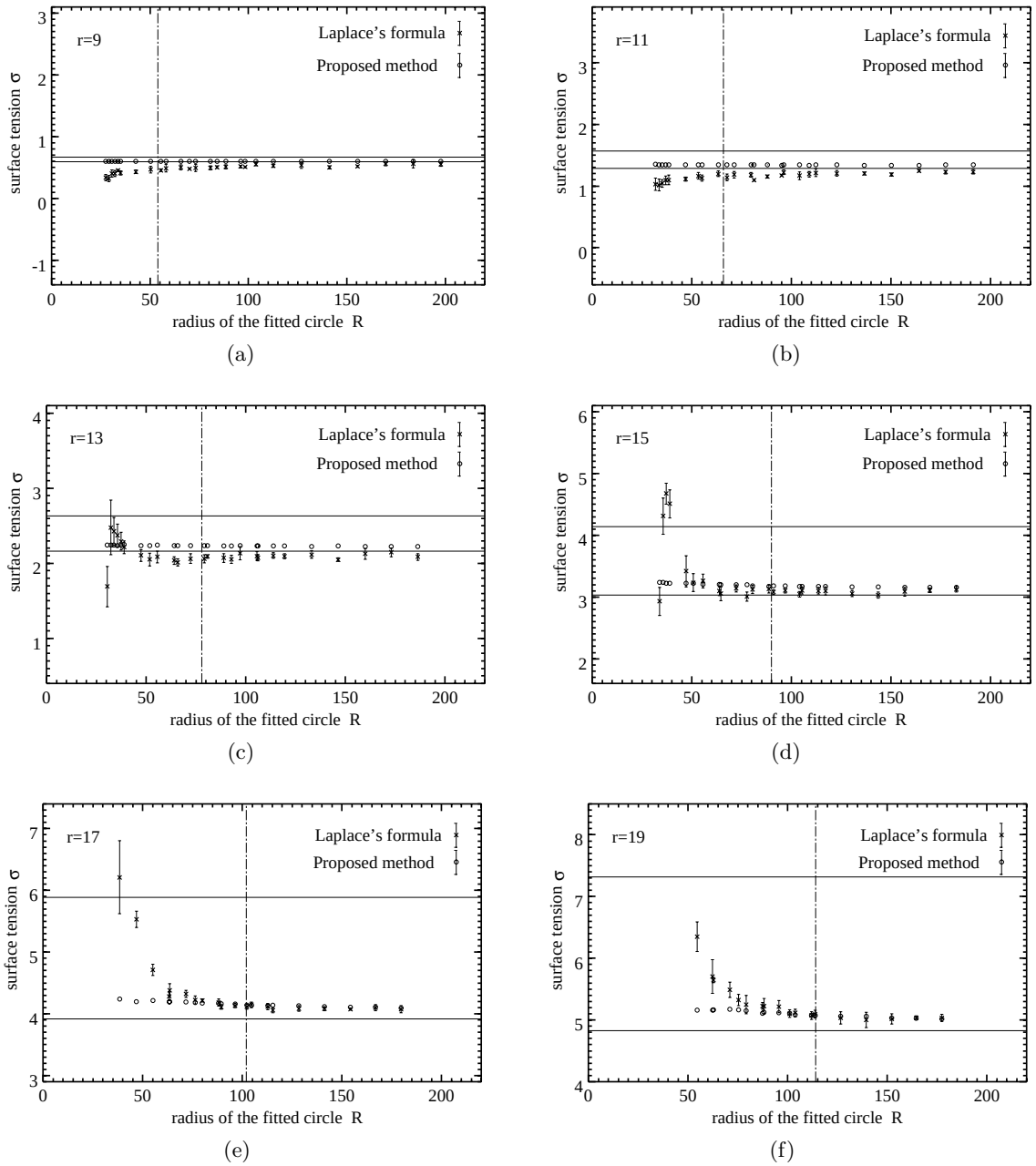

Fig. 8. Surface tension against the radius of the fitted circle: The surface tension of the droplet measured by using the Laplace's formula is plotted and the surface tension calculated by using the proposed method is also plotted as the small circle. The error bars of the calculated surface tension are less than 10^{-3} and smaller than the size of the small circle. The upper horizontal solid lines represent $\sigma_{\parallel}$ and the lower is for $\sigma_{\perp}$, and the vertical dash-dotted line represents $R = 6r$.

4.2.2 Measurement and comparison of the surface tension of the droplet

The surface tension of the droplet is measured by applying the Laplace's formula,

$$\sigma_{\rm c} = (p_{\rm in} - p_{\rm out})\ R, \tag{12}$$

where $p_{\rm in}$ and $p_{\rm out}$ are the pressures in the inside and the outside regions respectively. The radius R is obtained by fitting the mathematical circle to the interface position found by using the local-region clustering method in the previous section. The inside region and the outside region are defined as the region with the constant density and the constant mean free path. Then the region with the radius less than $R_s - 2r$ is regarded as the inside region and the region more than $R_s + 2r$ as the outside region, so that the surface thickness is $4r$ [17]. In other words, the surface tension is measured by ignoring the detail of the shape of the droplet surface.

In Figure 8, the surface tension measured by using the Laplace's formula (12) is plotted for $r = 9$ to $r = 19$ against the radius of the fitted circle. The size of the dense phase was varied by changing the lattice size from 200×200 to 700×700. For each lattice size, $d = 0.07$ and $d = 0.17$ were used as the reduced density of the system. The inside and the outside pressures were obtained by averaging 1200 steps in each simulation and the surface tension was obtained by averaging 5 simulations. In the figure, the surface tension of the droplet is not constant for the small radius because it is difficult to measure reasonable pressure in the small region. For the radius more than $6r$, which is represented by the vertical dash-dotted line, the surface tension of the droplet is almost constant. However it is found for $r = 15$, 17, and 19 that the surface tension of the droplet deviates from $\sigma_{\parallel}$ and $\sigma_{\perp}$ which are represented by the horizontal solid line.

Next, the method proposed in Section 3.2 is applied to the surface of the droplet. It is necessary that the surface obtained by using the local-region clustering method is smoothed partially to obtain the reasonable tangent. The coordinates of the point of contact is obtained by averaging over the coordinates of the continuous three nodes on the obtained surface. The slope of the tangent is also obtained as the slope of the line fitting to these three nodes. By applying this procedure and the proposed method to all of the surface nodes, it is determined whether the tangent at each surface node is parallel to the link direction or not. The ratio of the number of the surface node with the tangent parallel to the link direction to the number of the surface node gives the coefficient $\alpha_{\parallel}$ in equation (8). The surface tensions of both straight surfaces which are measured in Section 4.1 are used as $\sigma_{\parallel}$ and $\sigma_{\perp}$ in equation (8). The surface tension is calculated for each droplet surface of 5 simulations by the proposed method. The calculated surface tensions are averaged to obtain σ_{c}. In Figure 8, the obtained surface tension, σ_{c}, is also plotted as the small circle. It is found in the figure that the surface tension measured by using the Laplace's formula in the region of $R \geq 6r$ is in agreement with that calculated by the proposed method. The surface tension in the region of $R < 6r$, which cannot be obtained reasonably by using the Laplace's formula due to the small inside region, is also calculated by the proposed method.

5 Conclusion

A calculation method of the surface tension of the droplet in the liquid-gas model was proposed in consideration of the anisotropy of the surface tension because the shape of the droplet is determined by the Wulff construction and is not circular. The calculated surface tension of the droplet by the proposed method was in agreement with that measured by using the Laplace's formula in consideration of the surface thickness. According to Figure 8, it is found that the surface tension of the droplet was in agreement with neither $\sigma_{\parallel}$ nor $\sigma_{\perp}$ if the radius of the droplet approaches infinity. This difference increases as the distance of the long-range interaction is large.

Although $\sigma_{\parallel}$ and $\sigma_{\perp}$ are obtained by the numerical simulation in this paper, these may be derived by using the method by Appert and d'Humières [16]. The surface tension of the droplet could be calculated without numerical simulations. Since the proposed method gives the surface tension of the droplet as the combination of the surface tension of the straight surface, the surface tension of the part of the surface of the deformed droplet in flow fields can be calculated by the proposed method.

References

1. U. Frisch, B. Hasslacher, Y. Pomeau, Phys. Rev. Lett. **56**, 1505 (1986).
2. D.H. Rothman, S. Zaleski, Rev. Mod. Phys. **66**, 1417 (1994).
3. U. Frisch, D. d'Humières, B. Hasslacher, P. Lallemand, Y. Pomeau, J. Rivet, Complex Syst. **1**, 649 (1987).
4. L.B. Di Pietro, A. Melayah, S. Zaleski, Water Resource Research **30**, 2785 (1994).
5. K. Balasubramanian, F. Hayot, W.F. Saam, Phys. Rev. A **36**, 2248 (1987).
6. D.H. Rothman, J.M. Keller, J. Stat. Phys. **52**, 1119 (1988).
7. C. Appert, J.F. Olson, D.H. Rothman, S. Zaleski, J. Stat. Phys. **81**, 181 (1995).
8. J.F. Olson, D.H. Rothman, J. Stat. Phys. **81**, 199 (1995).
9. C. Appert, S. Zaleski, Phys. Rev. Lett. **64**, 1 (1990).
10. C. Appert, D.H. Rothman, S. Zaleski, Physica D **47**, 85 (1991).
11. C. Appert, D. d'Humières, V. Pot, S. Zaleski, Trans. Theor. Stat. Phys. **23**, 107 (1994).
12. L.D. Landau, E.M. Lifshitz, *Statistical Physics* (Pergamon Press, 1959).
13. J.S. Rowlinson, J. Stat. Phys. **20**, 197 (1979).
14. C. Appert, V. Pot, S. Zaleski, Fields Institute Commun. **6**, 1 (1996).
15. M. Gerits, M.H. Ernst, D. Frenkel, Phys. Rev. E **48**, 988 (1993).
16. C. Appert, D. d'Humières, Phys. Rev. E **51**, 4335 (1995).
17. K. Ebihara, T. Watanabe, H. Kaburaki, Int. J. Mod. Phys. C **9**, 1417 (1998).
18. C. Appert, S. Zaleski, J. Phys. II France **3**, 309 (1993).
19. R. Gomer, C.S. Smith, *Structure and properties of solid surfaces* (The university of Chicago press, 1953).
20. D. d'Humières, P. Lallemand, Complex Syst. **1**, 599 (1987).
21. C.A. Croxton, *Statistical Mechanics of The Liquid Surface* (John Wiley & Sons, 1980).